Theory of aging, rejuvenation, and the nonequilibrium steady state in deformed polymer glasses

Kang Chen[1] and Kenneth S. Schweizer[2,3,*]

[1]*Center for Soft Condensed Matter Physics and Interdisciplinary Research, Soochow University, Suzhou 215006, China*

[2]*Department of Materials Science, University of Illinois, 1304 West Green Street, Urbana, Illinois 61801, USA*

[3]*Kavli Institute of Theoretical Physics, University of California, Santa Barbara, California 93106, USA*

(Received 19 July 2010; published 20 October 2010)

The nonlinear Langevin equation theory of segmental relaxation, elasticity, and mechanical response of polymer glasses is extended to describe the coupled effects of physical aging, mechanical rejuvenation, and thermal history. The key structural variable is the amplitude of density fluctuations, and segmental dynamics proceeds via stress-modified activated barrier hopping on a dynamic free-energy profile. Mechanically generated disorder (rejuvenation) is quantified by a dissipative work argument and increases the amplitude of density fluctuations, thereby speeding up relaxation beyond that induced by the landscape tilting mechanism. The theory makes testable predictions for the time evolution and nonequilibrium steady state of the alpha relaxation time, density fluctuation amplitude, elastic modulus, and other properties. Model calculations reveal a rich dependence of these quantities on preaging time, applied stress, and temperature that reflects the highly nonlinear competition between physical aging and mechanical disordering. Thermal history is "erased" in the long-time limit, although the nonequilibrium steady state is not the literal "fully rejuvenated" freshly quenched glass. The present work provides the conceptual foundation for a quantitative treatment of the nonlinear mechanical response of polymer glasses under a variety of deformation protocols.

DOI: 10.1103/PhysRevE.82.041804 PACS number(s): 83.80.Ab, 64.70.Q−, 81.40.Cd, 83.50.−v

I. INTRODUCTION

Polymer liquids are ubiquitous glass formers due to their inherently slow kinetics and common inability to crystallize due to single chain structural disorder quenched in during chemical synthesis. Many aspects of their local dynamics in the supercooled melt are qualitatively similar to other glass formers, although distinctive effects arise associated with variable chain length and backbone stiffness, and also their possibility to spontaneously orient (liquid crystals) and mechanically deform in a moltenlike state (rubber networks) [1–5]. The alpha relaxation process occurs on the "statistical segment" (~nm) scale, which sets the elementary time scale for a hierarchy of relaxation processes associated with cooperative intrachain motions [6].

Polymers in the amorphous solid state (below T_g) are not only of scientific interest but also of great practical importance as engineering plastics [7–10]. Many new phenomena emerge: (i) the temperature dependence of the alpha time changes to a simpler Arrhenius form; (ii) physical aging is pervasive since most polymer glasses are used at temperatures not far below T_g; and (iii) mechanical deformation results in strain softening, yielding, local plastic flow, and strain hardening (a uniquely polymeric phenomenon) in a manner that depends strongly on temperature and strain rate. At lower strains ("preyield" regime), aging, thermal history, and mechanical response are coupled. However, at large ("postyield") strains, aging and thermal history are "erased" and a nonequilibrium steady state is achieved. How such relaxation and mechanical phenomena can be fundamentally understood at a segmental level is a major theoretical challenge.

Recent experiments on polymer glasses have revealed an intimate coupling between macroscopic nonlinear mechanical response in creep and relaxation on the local segmental scale [11–15]. A similar conclusion has been drawn from simulations [16–21], with segmental dynamics being surprisingly isotropic even under conditions of large strains before the hardening response emerges. These findings represent significant simplifications in the quest for a predictive theory of relaxation and nonlinear mechanics.

Building on a microscopic first-principles theory of activated barrier hopping, glassy dynamics, and nonlinear viscoelasticity of spherical particle liquids and colloidal suspensions [22–25], we recently proposed and widely applied a lightly coarse-grained segmental scale statistical mechanical approach for cold polymer liquids and glasses [26–35]. The key slow dynamical variable is the experimentally observable collective density fluctuation amplitude on segmental and beyond length scales. Barrier hopping is described based on the concept of a local dynamic free energy which is determined by structural properties and thermodynamic state. Physical aging has been addressed in the absence of mechanical deformation [29,30], and a constitutive equation for nonlinear mechanical response developed in the absence of aging and mechanical disordering ("rejuvenation") [31,32]. This theoretical work has been recently reviewed [36,37].

Despite significant successes, a unified nonlinear Langevin equation (NLE) description that simultaneously includes aging, deformation lowering of activation barriers, and mechanical rejuvenation does not exist. Hence, phenomena such as the "yield stress peak," "strain softening," erasure of aging, and the full nature of the steady state plastic flow regime have not been addressed. The goal of the present work is to propose the conceptual generalization of our polymer glass theories to treat these more complex issues. Given the high difficulty of this nonequilibrium statistical physics problem, we are guided by a combination of hints gleaned from ex-

*kschweiz@illinois.edu

periment, simulation and ideas proposed in the context of the shear transformation zone (STZ) theory of atomic glass plasticity [38].

Section II recalls relevant aspects of prior work. A quantitative model for the combined effects of mechanical disordering, aging, and constitutive response is formulated in Sec. III. Model calculations are presented in Sec. IV to illustrate key predicted trends. The paper concludes in Sec. V with a summary and future outlook.

II. THEORETICAL BACKGROUND

We briefly discuss the prior work that provides the foundation for our extensions. Detailed explanation of both the theoretical concepts and technical approximations are given in the literature and two review articles [36,37].

A. Basics and quiescent supercooled melts

The NLE theory of glassy polymer dynamics is formulated at a lightly coarse-grained statistical segment level [26]. It is a simpler analytic version of the fully microscopic formulation that has been widely applied to dense particle fluids and colloidal suspensions [22–25]. Segments represent a collection of a few real monomer units and have a size $\sigma = \sqrt{C_\infty} l_b$, where l_b is the chemical backbone bond length ($\sim$0.15 nm) and $C_\infty \sim 4-10$ is the characteristic ratio. Dynamical degrees of freedom are separated into two categories: (i) very local and fast (intrasegment scale) motions which are treated in an irreversible manner via a friction constant (ζ_s) or "bare" Arrhenius relaxation time scale, $\tau_0(T) \equiv \tau_0 \exp(\varepsilon_A / k_B T)$ ($\tau_0 \approx 10^{-14\pm1}$ s is a vibrational time scale, and ε_A a local activation energy), and (ii) the slower segmental scale degrees of freedom which define the alpha relaxation. Segmental dynamics is described by a stochastic NLE formulated based on dynamic density functional and local equilibrium ideas [23,26,36],

$$\zeta_s \frac{\partial r_\alpha(t)}{\partial t} = -\frac{\partial F_{eff}[r_\alpha(t)]}{\partial r_\alpha(t)} + \delta f_\alpha(t), \tag{1}$$

where $r_\alpha(t)$ is the absolute value of the displacement of segment α from its initial ($t=0$) position, the white-noise random force satisfies $\langle \delta f_\alpha(0) \delta f_\alpha(t) \rangle = 2 k_B T \zeta_s \delta(t)$, and the "dynamic free energy" is the key quantity which describes an effective force exerted by the surroundings and is given by

$$\beta F_{eff}(r) = -3\ln(r) - \int \frac{d\vec{q}}{(2\pi)^3} \rho C_0^2 S(q)[1+S(q)]^{-1} \times \exp\left\{ -\frac{q^2 r^2}{6}[1+S^{-1}(q)] \right\}, \tag{2}$$

where $\beta \equiv (k_B T)^{-1}$ is the inverse thermal energy. The first term can be thought of as an ideal entropy like contribution that favors delocalization (liquid state), or more accurately describes a short-time Fickian diffusion process in Eq. (1) presumed to describe the irreversible highly local dynamics at small segmental displacements [23,37]. The second "caging" term describes the effect of interpolymer forces which favors segmental localization (glass state). Subnanometer structural and interaction potential length scales are averaged over at the statistical segmental scale, resulting in a site-site direct correlation function $C(q) = C(q=0) = C_0$ and collective density fluctuation structure factor given by $S^{-1}(q) = S_0^{-1} + \frac{1}{12} q^2 \sigma^2$. Under equilibrated conditions the latter are time-independent structural or thermodynamic quantities, where $S_0 = \rho k_B T \kappa = (-\rho C_0)^{-1}$ is the dimensionless isothermal compressibility that quantifies the amplitude of thermal density fluctuations on nanometer and beyond scales, κ is the isothermal compressibility, and $\rho\sigma^3$ is the reduced segmental density. Theory and experiment suggest that $S_0^{-1/2} = -A + (B/T)$, where $A > 0$ and B correlates with monomer cohesive energy [26]. At the segmental level, $F_{eff}(r)$ is determined for long chains by a single material-specific "coupling constant"

$$\lambda \equiv (\rho \sigma^3 S_0^{3/2})^{-1}, \tag{3}$$

which increases with cooling or pressure and involves only measurable equilibrium quantities.

Equations (1)–(3) predict a dynamical crossover at $\lambda_c = 8.32$ where F_{eff} first acquires a "localized form" with a minimum (at a localization length, r_{loc}) and barrier (F_B). This crossover defines a naive mode coupling theory (MCT) [26,39] "ideal glass transition" at $T_c = B[A + (\lambda_c \rho \sigma^3)^{1/3}]^{-1}$. The focus of NLE theory is the *deeply* supercooled regime where numerical calculations of barriers are well represented as $\beta F_B \simeq c(\lambda - \lambda_c)^\Delta$, $c \sim 0.4$, and $\Delta \cong 1.4$. Given the complexity of polymeric liquids (including the fast relaxation process) and the lightly coarse-grained segmental description adopted, we do not numerically solve stochastic evolution equation (1). Rather, as thoroughly discussed and physically motivated previously [26,36,37], we implement a simpler analytic approach which employs only the dynamic free energy barrier computed using Eq. (2). Specifically, a mean hopping or alpha time, $\tau_\alpha(T)$, is determined in a Kramers-like manner [26],

$$\tau_\alpha(T) = \tau_0 \exp\left(\frac{\varepsilon_A}{k_B T}\right) \exp\left[\frac{a_c F_B(T)}{k_B T}\right]. \tag{4}$$

The local activation energy is determined by adopting the recent proposition [40] of a (nearly) universal dynamical crossover time: $\tau_0(T_c) \equiv \tau_0 \exp(\varepsilon_A / k_B T_c) \cong 10^{-7\pm1}$ s. Short-range intrachain correlations due to backbone stiffness are expected to introduce a cooperativity of the hopping event which is crudely modeled in Eq. (4) via a material-specific temperature-*independent* parameter, a_c, which is the number of dynamically correlated segments along the chain and is *a priori* estimated to be $a_c \sim 1-8$ [28]. NLE theory predicts sensible values for T_c, and also T_g based on the experimental criterion $\tau_\alpha(T_g) = 10^x$ s, where $x = 2-4$. The glassy elastic shear modulus G' due to *interchain* stresses can be calculated using a standard Green-Kubo formula [34,37],

$$G' = \frac{k_B T}{60\pi^2} \int_0^\infty dq \left\{ q^2 \frac{d}{dq} \ln[S(q)] \right\}^2 e^{-q^2 r_{loc}^2 / 3S(q)}. \tag{5}$$

Young's modulus follows as $E' \simeq 2.8 G'$ [31].

B. Relaxation and physical aging below T_g

Extension of NLE theory to below T_g assumes that the dimensionless density fluctuation amplitude remains the relevant slow variable and caging constraints are quantified by its *nonequilibrium* value which becomes time dependent if aging occurs [34]. From a potential energy landscape (PEL) perspective, density fluctuations have two contributions: vibrational motions (intrabasin) which remain equilibrated at temperature T and larger scale structural rearrangements (interbasin) which fall out of equilibrium below T_g [41,42]. After a rapid quench, the temperature dependence of S_0 changes and scattering experiments are well represented as (a) $S_0 \propto T$ sufficiently far below T_g as in a harmonic solid and (b) saturation at a nonzero value as $T \to 0$ due to frozen-in density fluctuations, $S_0(T \to 0) \equiv bS_0(T_g)$, where experimentally $b \sim 0.4-0.75$. This motivates a minimalist form in the *quenched* glass [34],

$$S_0(T) = bS_0(T_g) + \frac{T}{T_g}(1-b)S_0(T_g), \tag{6}$$

where the second (first) term is the contribution from the fast (slow) degrees of freedom. In the absence of aging, the theory predicts an Arrhenius-like temperature dependence of the segmental relaxation time, in accord with many experiments [34].

The amplitude of density fluctuations, which is the fundamental structural variable that determines the mean segmental relaxation time, becomes time dependent under nonequilibrium aging conditions. A first-order kinetic model [29,30] is employed to describe the time evolution of $S_0(t)$ from its nonequilibrium quenched value ($t=0$) to the smaller equilibrium value, $S_{0,l}$,

$$\frac{dS_0(t)}{dt} = -\frac{S_0(t) - S_{0,l}}{\tau_\alpha(t)}. \tag{7}$$

This rate equation actually describes the time evolution of the slow configurational part of the density fluctuation amplitude, $\Delta S_0(t) \equiv S_0(t) - (T/T_g)(1-b)S_0(T_g)$. The physical idea is equilibration "down the landscape" proceeds via activated hopping which is self-consistently determined by $S_0(t)$ via Eqs. (3), (4), (6), and (7). Only experimentally measurable quantities enter, and the solution of Eq. (7) is of an "effective time" form: $S_0(t) - S_{0,l} = [S_0(0) - S_{0,l}]\exp\{-\int_0^t [dt'/\tau_\alpha(t')]\}$. An "effective temperature" idea is not invoked, but a fictive temperature can be computed postfacto [29]. On intermediate time scales, the theory predicts logarithmic aging of thermodynamiclike properties and apparent power-law aging of the alpha relaxation time, $\tau_\alpha(t) \propto t^{\mu(T)}$, in good agreement with polymer experiments [29,30]. Note that since the relaxation time and S_0 are directly coupled via the barrier height, our aging theory can also be thought of as formulated in terms of an evolution equation for the segmental relaxation time.

C. Effect of applied stress

External stress is modeled via an *instantaneous* dynamical variable analog of the Eyring landscape tilting idea [43–45]. Stress introduces an anisotropic bias which lowers activation barriers corresponding to a direct mechanical acceleration of relaxation. In the spirit of the MCT of rheology [46] and early soft glassy rheology models [47], the stress-induced force is modeled in a spatially isotropic manner. Such a simplification is supported by simulations which find local glassy relaxation is massively sped up by stress but in a nearly isotropic fashion [17,19]. This physical picture implies that the dynamic free energy acquires a new term of a mechanical work form [35,48],

$$F_{mech}(r) = -f \cdot r, \quad f = c\sigma^2\tau, \tag{8}$$

where τ is applied stress and c is a constant of order unity. Stress reduces the barrier and accelerates relaxation but with multiple non-Eyring features [35]. The barrier is destroyed at an "absolute yield stress," τ_{abs}, whence cage escape no longer requires thermal activation in the manner of an "athermal" or "granular" limit. Stress also increases the localization length, thereby reducing the elastic modulus in Eq. (3).

In this zeroth-order model the coupling constant of Eq. (3) is assumed to be unmodified by deformation, and thus mechanical rejuvenation effects are ignored. The fast relaxation time scale, $\tau_0(T)$, is also assumed to be deformation and age independent. Theoretical predictions for the initial reduction of τ_α under moderate stress agree well with experiments and simulations, but large deviations emerge in the postyield regime associated with the onset of plastic flow and strain hardening [10,20].

D. Constitutive equation

Under quenched conditions (no aging or mechanical rejuvenation), a generalized Maxwell constitutive equation has been proposed where the only input is the stress-dependent elastic modulus and mean segmental relaxation time [31],

$$\tau(t) = \int_0^t E(t-t')\dot{\gamma}(t')dt', \tag{9}$$

where $\dot{\gamma}(t)$ is a time-dependent strain rate. The deformation-dependent modulus obeys

$$\frac{dE[t;\tau(t)]}{dt} = -\frac{E[t;\tau(t)]}{\tau_\alpha[\tau(t)]} \tag{10}$$

and hence

$$\tau(t) = \int_0^t dt' E'[\tau(t')]\exp\left\{-\int_{t'}^t dt'' \tau_\alpha^{-1}[\tau(t'')]\right\}\dot{\gamma}(t'). \tag{11}$$

Equation (11), plus the stressed versions of Eqs. (4) and (5), comprises a self-consistent nonlinear description of mechanical response, elasticity, and relaxation. For a constant rate experiment the strain $\gamma = \dot{\gamma}t$, and the stress-strain relation is

$$\tau(\gamma) = \int_0^\gamma d\gamma' E'(\gamma')\exp\left\{-\int_{\gamma'}^\gamma d\gamma'[\dot{\gamma}\tau_\alpha(\gamma')]^{-1}\right\}. \tag{12}$$

Plastic flow, as defined by a constant steady-state stress at large times (strains) in the absence of strain hardening, cor-

responds to a dynamic yield or plastic flow stress self-consistently determined by

$$\tau_y = \dot{\gamma} E'(\tau_y)\tau_\alpha(\tau_y). \quad (13)$$

Detailed calculations of stress-strain curves for polymethylmethacrylate (PMMA) show that the experimental deformation behavior is well described under rapidly quenched conditions [31]. However, if the latter is relaxed, then the theory does not capture the experimentally observed local maximum (stress overshoot) and strong preaging effects.

The theory has also been worked out for constant stress creep experiments [32], and good agreement is found under preflow conditions [32]. But, the massive increase of stress observed in polymer glasses at high strains is not captured. A successful theory for this nonentropic strain hardening phenomenon has been formulated based on the idea that it is a consequence of prolongation of τ_α and increase of flow stress due to anisotropic chain deformation and packing [33]. How strain hardening is modified by aging and rejuvenation is not addressed in this paper.

E. Open issues and theoretical approach

Our prior theoretical work has achieved significant understanding of the relaxation and nonlinear mechanical response under rapidly quenched and no aging conditions [36,37]. However, the following important physical effects have not been treated, and addressing them is our present goal. (1) Incorporation of a quiescent thermal history before a mechanical test is performed. What is the role of waiting (*preaging*) time and quench depth? (2) Inclusion of aging *during* a nonlinear mechanical experiment. When is this important? (3) Formulation of a theory for stress-induced enhancement of density fluctuations, i.e., mechanical rejuvenation. (4) Related issues include (i) how deformation modifies aging in the preyield versus postyield regimes; (ii) how rejuvenation, aging, and strain rate couple to determine the nonequilibrium steady state; and (iii) how the latter is related to the quenched material. Note that mechanical deformation influences the dynamic free energy in two distinct manners: (a) a "passive" direct landscape tilting as in Sec. II C, and (b) an active change via mechanical modification of S_0 (rejuvenation).

Although the full numerical stochastic NLE approach includes dynamic heterogeneity (DH) effects [23–25], we adopt the mean-field framework underlying the analytic polymer version of theory [26–28,36,37] and do not consider a relaxation time distribution. This effectively homogenous view is typical of effective time theories traditionally employed for polymer glasses [4,8,49]. It can be contrasted with "defect" models formulated in terms of a small population of mobile "excitations" (which may [50–52] or may not [38,53,54] be strictly conserved) embedded in a sea of immobile regions, examples of which include shear transformation zones [38], diffusing and dynamically facilitating defects in kinetically constrained models [50–52], and a percolation free volume model based on "liquid" and "solid" cells [55]. The localized defects are not equilibrium objects but exist in a temporally coarse-grained sense as particle configurations that cost energy to create which serve as transition states for relaxation and plasticity. Their concentration is usually postulated to obey a Boltzmann-like distribution, and the defects may interact via elastic mediation and/or spatial diffusion in various assumed manners.

Reality is likely intermediate between the homogeneous and heterogeneous defect pictures. The former view seems more appropriate not far below T_g (where polymer glasses are generally studied), while the latter may be more appropriate far below T_g (where metallic glasses are generally studied). In both STZ theory and our approach, stress lowers barriers, enhances mobility or defect concentration, and can lead to a mechanically induced glass-to-liquid transition. Regarding dynamic heterogeneity effects, on the experimental mean alpha time scale the system is in the process of transforming from a dynamically heterogeneous regime where mobility is spatially distributed to a dynamically uniform relaxed material where a spatially homogeneous picture applies. In other words, the lifetime of dynamic heterogeneity and mean alpha time are generally believed to comparable, although this remains a question of active investigation.

III. COUPLED MECHANICAL REJUVENATION AND PHYSICAL AGING

A deep statistical physics question is how a nonequilibrium system dynamically navigates the PEL under the combined action of aging and mechanical agitation. The goal of approximate theory is to identify a structural variable(s) which adequately captures such complexity. We present a minimalist extension of the polymeric NLE theory to include the combined consequences of aging and rejuvenation on relaxation and mechanics. A rigorous statistical mechanical approach is intractable, and we are guided by insights gleaned from experiment, simulation, and plasticity theories for atomic materials [38].

A. Background and motivation

Recent stress-controlled simulations have provided considerable insight to the relevant physics in aging and mechanically deformed glasses within the PEL framework [44,45,56]. Stress not only introduces a tilt to the PEL in the direction of positive strain but also introduces extra disorder that enhances mobility, and thus two types of thermally activated processes can be identified. (1) In the aging glass, activated events move the system "down" the PEL. The hopping rate in the presence of stress controls mechanical relaxation and is enhanced via tilting of the PEL. (2) At large enough stresses, activated transitions are more directly driven mechanically as a consequence of the system being "pushed up" the PEL. Thermodynamically based effective temperature models for aging and deformed glasses are being developed in the context of STZ theory [57], where the second process is interpreted as a "mechanical stirring" effect corresponding to a stress-induced enhancement of configurational disorder at the inherent structure level resulting in faster relaxation. Similar, but cruder, physical ideas were invoked long ago by Spaepen for metals [53], Struik for polymers [8], and others where deformation creates free volume

and enhances mobility. We adapt the above qualitative picture in the context of NLE theory, and the central task is how rejuvenation and aging physics is encoded in the nonequilibrium evolution equation for our structural variable, $S_0(t)$.

As relevant background, we first recall how aging and disorder production is described by Struik [8,52] for polymers within the free volume framework (V_f),

$$\frac{dV_f}{dt} = -\frac{V_f - V_\infty}{\tau_\alpha(V_f)} + Q(V_f), \tag{14}$$

where the first term on the right-hand side (RHS) describes aging to equilibrium and the second term ($Q>0$) describes free volume production [58]. The latter is taken to be proportional to the rate of mechanical energy dissipation, and in practice Q scales as the absolute value of the strain rate to the *first* power. Lee and Ediger [15] recently confronted this description with polymer glass mobility measurements and found strong deviations. Moreover, Langer [38] emphasized that a free volume production term linear in strain rate violates the basic requirement that it is an even function of $\dot{\gamma}$. Mechanical-induced disordering has also been studied for a variety of complex fluids (colloids, pastes, and gels) that exhibit glasslike dynamics based on a highly phenomenological evolution equation for a (usually vaguely defined) structural variable, $A(t)$, given by [59]

$$\frac{dA}{dt} = -\tau_\alpha^{-1} + bA\dot{\gamma}, \tag{15}$$

where b is a numerical factor. Typically, no precise definition is given for the system-specific A variable, although free volume is one example [59]. The first term on the RHS of Eq. (15) describes a simplified aging model which, as in Eq. (14), is based on a *quiescent* relaxation time. The last term describes disorder production which scales linearly with strain rate. One expects that Eq. (15) shares similar limitations as Eq. (14) and is subject to the same Langer criticism. However, as also done in STZ theory [38], these phenomenological theories both assume that the relaxation time that enters the aging term does *not* depend on deformation.

We propose to treat mechanical rejuvenation via an enhancement of the density fluctuation amplitude in the dissipated power framework as employed by Langer [38]. States of larger S_0 (more disordered) are accessed via activated hopping at a stress-dependent rate. There is an "end point" to this process, corresponding to a "fully rejuvenated state" for which there is no consensus definition. Our prior work was implicitly consistent with Langer who defines this state in the limit of low $\dot{\gamma}$ and temperature where the competing aging process is absent, and the limiting reference state is assumed to be a glass with the degree of structural disorder frozen in at T_g. Thus, we do not distinguish between the freshly quenched and fully rejuvenated states [60]. Note that the literal full rejuvenation hypothesis [8] does not apply at nonzero temperature or strain rate where aging occurs in parallel with mechanical stirring. We continue to assume the fast relaxation process is unaffected by deformation and aging, so these degrees of freedom serve as an equilibrated heat bath for the slow alpha relaxation process.

We conclude this motivation section by noting an important polymer glass scattering experiment that measured S_0 under deformation and found an increase of the density fluctuation amplitude with stress [61]. This provides direct support for our use of a mechanically enhanced density fluctuation amplitude as a relevant and experimentally observable structural variable. Indirect support comes from positron annihilation lifetime spectroscopy experiments which deduce "free volume" (loosely related to density fluctuations) is enhanced upon application of stress [62]. Direct evidence for mechanical disordering of glass structure is also emerging for amorphous metals based on measurements of the full $S(q)$ [63].

B. Rejuvenation model

We assume that the rate at which density fluctuations are mechanically enhanced is proportional to the dissipative mechanical work and grows linearly with the departure from the freshly quenched value, $S_{0,g}$,

$$\frac{dS_0}{dt} = \psi(S_{0,g} - S_0)\tau\dot{\gamma}, \tag{16}$$

where ψ is an of order unity (*a priori* unknown) numerical prefactor in units of inverse stress, $(k_BT/\sigma^3)^{-1}$. Equation (16) obeys the minimal constraint that the density fluctuation production rate is an even function of deformation rate [38]. Recall that this equation really describes the evolution of the slow configurational part of density fluctuations, $\Delta S_0(t) \equiv S_0(t) - (T/T_g)(1-b)S_0(T_g)$, since the fast vibrational part is equilibrated and unaffected by stress. Formally integrating Eq. (16) yields

$$S_0(t) = S_{0,g} - (S_{0,g} - S_{0,i})\exp\left(-\psi\int_0^{\gamma(t)} \tau d\gamma\right), \tag{17}$$

where $S_{0,i}$ denotes the value of S_0 at the start of the mechanical experiment after a preaging time interval. The degree of rejuvenation depends on the total amount of mechanical work, $\int_0^{\gamma(t)} \tau d\gamma$, a counterintuitive consequence of which is that recoverable deformation can cause rejuvenation. For example, upon applying a step stress, the instantaneous elastic step strain can induce rejuvenation in Eq. (17). A physically motivated solution to this "problem," consistent with only the slow configurational part of S_0 undergoing nonequilibrium dynamics, is to replace the total deformation rate with its irreversible *dissipative plastic analog*, which follows from Eq. (13) as [31]

$$\dot{\gamma}_{pl} = \tau/[E'(\tau)\tau_\alpha(\tau)], \tag{18}$$

thereby yielding

$$\frac{dS_0}{dt} = \psi(S_{0,g} - S_0)\tau^2/[E'(\tau)\tau_\alpha(\tau)]. \tag{19}$$

The solution of Eq. (19) can be formally written as

$$S_0(t) = S_{0,g} - (S_{0,g} - S_{0,i})\exp\left\{-\psi\int_0^t \tau^2/[E'(\tau)\tau_\alpha(\tau)]dt'\right\}, \tag{20}$$

where stress depends implicitly on time in a constant rate experiment but is fixed in a creep experiment. Predictions of Eq. (20) depend on the initial aged state and deformation details. Our description of rejuvenation is broadly in the spirit of Langer's STZ plasticity theory [38] based on flow defects and an effective temperature, although the latter two constructs do not enter our spatially homogeneous "effective relaxation time" approach.

C. Physical aging in the presence of stress

How stress affects aging is a longstanding and controversial question [8,64]. Polymer experiments by McKenna [64] have shown that under low stress preyield conditions there is no change of thermodynamic state in the sense that the aging equilibration time is unperturbed even though the mechanical relaxation time can be dramatically reduced (presumably via landscape tilting). This view is consistent with the recent experimental findings that increase of the segmental relaxation time with aging and decrease with applied stress are effectively independent or additive processes [15].

For large deformations little is fundamentally understood. Phenomenological theories of many types [e.g., Eqs. (14) and (15); STZ theory [38]] typically assume such a separation of aging and mechanical disordering still holds *at the level* of the time-evolution equation for the structural variable. The relaxation time that quantifies the rejuvenation process involves stress-dependent activated hopping, while aging is controlled by a barrier characteristic of the quiescent glass. We adopt this zeroth-order picture, and thus the driving force for reduction of S_0 remains the same as in Eq. (7),

$$\frac{dS_0}{dt} = \psi(S_{0,g} - S_0)\tau^2/[E'(\tau,S_0)\tau_\alpha(\tau,S_0)] - (S_0 - S_{0,l})/\tau_\alpha(0,S_0), \tag{21}$$

where $S_0(t=0)=S_{0,i}$.

D. Nonequilibrium steady state

There remains the question as to what is the nature of the long time nonequilibrium steady state. We do not assume that the glass is fully rejuvenated but rather use Eq. (21) to self-consistently determine the optimum balance of aging and mechanical disordering. This issue is relevant to the "viscosity bifurcation" [59] phenomenon in soft glassy materials. Here, as a function of applied stress and preaging aging protocol, the question is whether the relaxation time appears to grow in an unbounded manner at long elapsed times ("aging wins") or whether it saturates at a smaller value than before the deformation was applied ("rejuvenation wins"). Which type of steady state occurs depends on system details: temperature, applied stress level, and length of preaging. The final stationary steady-state value of $S_0(t\to\infty)\equiv S_{0,\infty}$ follows from Eq. (21) as

$$S_{0,\infty} = \frac{\psi\tau^2\tau_\alpha(0,S_{0,\infty})S_{0,g} + E'(\tau,S_{0,\infty})\tau_\alpha(\tau,S_{0,\infty})S_{0,l}}{E'(\tau,S_{0,\infty})\tau_\alpha(\tau,S_{0,\infty}) + \psi\tau^2\tau_\alpha(0,S_{0,\infty})}. \tag{22}$$

This result is independent of the degree of preaging, and hence thermal history is erased at long times. Equation (22) is a nonlinear self-consistent equation for $S_{0,\infty}$ that requires knowledge of the elastic modulus of Eq. (5), relaxation time of Eq. (4), equilibrium S_0 and applied stress, which in turn follow from the coupling constant λ of Eq. (3), the dynamic free-energy localization length and barrier, and the constitutive relation of Eq. (11).

For a constant strain rate experiment, the nonequilibrium steady state corresponds to a constant plateau flow (or dynamic yield) stress, given by the self-consistent relation

$$\tau_y = \dot\gamma E'(\tau_y,S_{0,\infty})\tau_\alpha(\tau_y,S_{0,\infty}), \tag{23}$$

which is coupled with Eq. (22) and depends on $\dot\gamma$. Equation (22) then simplifies to

$$S_{0,\infty} = \frac{\lambda\tau_y\dot\gamma\tau_\alpha(0,S_{0,\infty})S_{0,g} + S_{0,l}}{1 + \lambda\tau_y\dot\gamma\tau_\alpha(0,S_{0,\infty})}. \tag{24}$$

Since τ_y and $\dot\gamma\tau_\alpha(0,S_{0,\infty})$ both increase with strain rate [31], in a hypothetical high strain rate limit the fully rejuvenation result is obtained: $S_{0,\infty}\to S_{0,g}$.

E. Modified constitutive equation

The form of the constitutive equation in Sec. II D is unchanged. Extra complexity enters only via the effects of aging and rejuvenation on $S_0(t)$ which are nonlinearly coupled with the stress or strain evolution equation. The molecularly well-defined parameters that enter the extended NLE theory are unchanged except for specification of the numerical prefactor, ψ, in Eq. (16). Under a constant strain rate deformation, Eq. (12) still applies. For constant stress creep deformation, our prior Maxwell model theory remains unchanged in form [32]

$$\gamma(t) = \gamma_0 + \int_0^t dt' \frac{\tau}{E'(\tau,t')\tau_\alpha(\tau,t')},$$

$$\gamma_0 \equiv \int_0^\tau d\tau'/E'(\tau',0). \tag{25}$$

The long time viscous flow limit can be characterized by a limiting strain rate

$$\dot\gamma_\infty \to \frac{\tau}{E'(\tau,S_{0,\infty})\tau_\alpha(\tau,S_{0,\infty})} \equiv \frac{\gamma_y}{\tau_\alpha(\tau,S_{0,\infty})}, \tag{26}$$

where the last equality defines an apparent yield strain.

IV. MODEL CALCULATIONS

We now present model calculations within a stress-control framework of fundamental measurable quantities that characterize the nonequilibrium dynamics. Our goal is to show

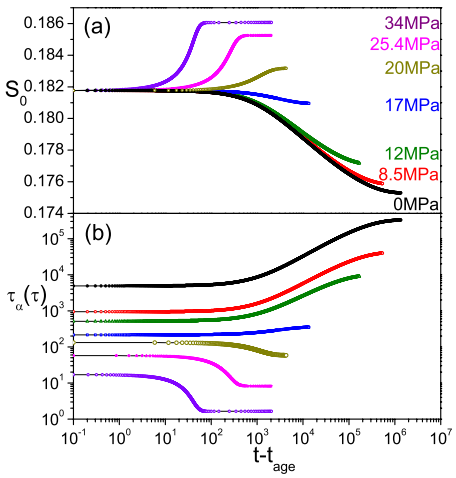

FIG. 1. (Color online) Time evolution of (a) density fluctuation amplitude, $S_0(t)$, and (b) mean relaxation time (in seconds), $\tau_\alpha(t)$, under the indicated constant stresses which increase (decrease) from bottom to top for $S_0(t)$ [$\tau_\alpha(t)$] and for fixed $T=T_g-10$ K (shallow quench) and preaging time $t_{age}=10^3$ s (short).

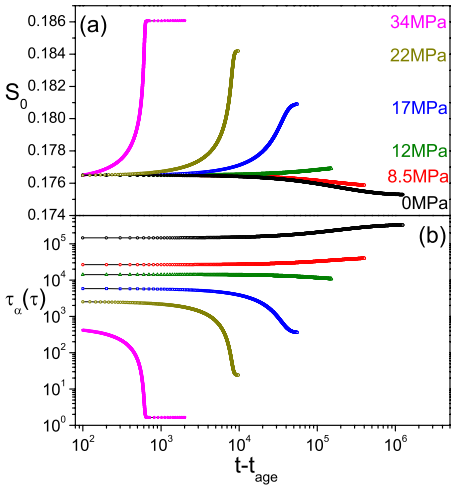

FIG. 2. (Color online) Same as Fig. 1 but for $T=T_g-10$ K (shallow quench) and $t_{age}=10^5$ s (long).

representative examples of the predicted rich competition between aging and rejuvenation with regard to determining the dynamic evolution and steady state of the density fluctuation amplitude, relaxation time, flow stress, creep strain rate, and bifurcation phenomenon. All computations are done for a single set of material properties previously developed [31] to describe PMMA glass [65], with $\psi^{-1}=k_BT/\sigma^3$ in Eq. (16). The control parameters are temperature, applied stress, and preaging time.

We remind the reader that here we focus solely on the competition between aging and rejuvenation and ignore strain hardening and chain entanglement effects. Our calculations are relevant to a plastic flow regime where the stress is (nearly) constant corresponding to strains beyond a "yield peak" (typically $\sim 5-10$ % strain) but below the onset of chain deformation and hardening at much higher strains [9,10].

A. Dynamic evolution of density fluctuation amplitude and alpha time

The nonequilibrium evolution of the density fluctuation amplitude and relaxation time depend on the preaging time and applied stress. Results are shown in Figs. 1–4 as a function of stress for two temperature quenches (shallow, $\Delta T \equiv T_g - T = 10$ K, and deep, $\Delta T \equiv T_g - T = 50$ K) and two preaging times (short, $t_{age}=1000$ s, and long, $t_{age}=10^5$ s). All curves are sigmoidal-like. The relaxation time can either strongly increase with elapsed time ($t-t_{age}$) or decrease with time and saturate, depending on the stress, quench depth, and preaging time. The shape of the curves is reminiscent of the down versus up jump asymmetric quiescent aging behavior discussed previously [29]. For example, when S_0 (τ_α) decreases (increases) with elapsed time, typically a logarithmic (effective power law) form applies on intermediate time scales. On the other hand, when S_0 (τ_α) grows (decreases) with elapsed time, the dynamical evolution is much more abrupt and does not follow any simple power law or logarithmic scaling.

We now discuss the results in detail. Consider first the two shallow quench cases (Figs. 1 and 2). With increasing stress, τ_α and S_0 monotonically decrease and increase, respectively, and the nonequilibrium steady state (saturation of the curves) is attained at shorter elapsed times. Note the remarkably small changes in S_0 relative to the many orders of magnitude change of the relaxation time. This is a hallmark of the glass problem where small structural changes have very large dynamical consequences. Now, in the low stress regime for the short preaging time (Fig. 1), S_0 is essentially unchanged by deformation even though τ_α is significantly decreased and follows an intermediate time power-law growth with an apparent exponent that is essentially independent of stress. This corresponds to an Eyring-like behavior discussed previously [31,35] where rejuvenation effects are unimportant and physical aging is dominant. Beyond a critical stress, which is lower for longer t_{age} (Fig. 2), the time-evolution curves qualitatively change signaling a crossover to a regime where mechanically induced disorder "wins." This crossover de-

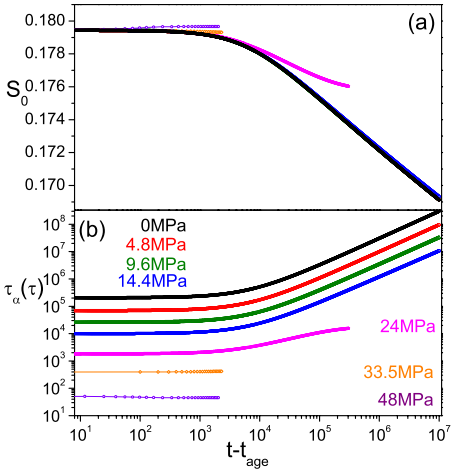

FIG. 3. (Color online) Same as Fig. 1 but for $T=T_g-50$ K (deep quench) and $t_{age}=10^3$ s (short).

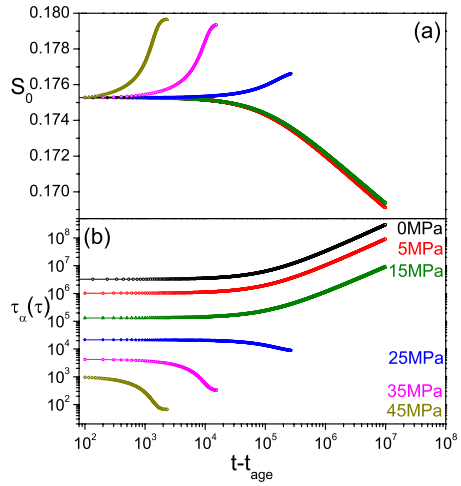

FIG. 4. (Color online) Same as Fig. 1 but for $T=T_g-50$ K (deep quench) and $t_{age}=10^5$ s (long).

fines a dynamic yield stress or bifurcation of the nonequilibrium dynamics, where the bifurcation stress is smaller for the longer preaged systems. At high stresses, the steady-state value of S_0 approaches, but is not exactly equal to, the quenched glass value that defines the fully rejuvenated state. Qualitatively, the evolution with stress of the relaxation time and bifurcation signatures agree with experiments on glassy complex fluids [59]. However, note that in the low stress regime the relaxation time does not literally diverge but rather simply becomes too long to be experimentally observable; there are no finite temperature divergent relaxation times in our theoretical approach.

Figures 3 and 4 show analogous results for a much deeper temperature quench. At fixed preaging time, note the significant quantitative differences compared to the shallow quench behavior in Figs. 1 and 2. However, globally the type of dynamical behaviors that occur as stress and preaging time are varied is similar.

B. Dynamic yield or bifurcation stress

A dynamic yield stress, τ_{dy}, can be precisely defined as the critical stress that separates the "aging wins" versus "rejuvenation wins" time evolution of the relaxation time. Calculations of this quantity as a function of quench depth for five experimentally relevant preaging times are shown in Fig. 5. Note that an apparent threshold temperature is required to observe dynamic yielding, which increases with t_{age}. Globally, all curves have the same shape and exhibit three regimes: (i) roughly linear growth for small values of $\Delta T \equiv T_g - T$, (ii) crossover to a slowly varying dependence at intermediate values of ΔT, and (iii) upturn at large quench depths.

The magnitudes of τ_{dy} are much smaller than the linear elastic modulus (~GPa) and of the same order of magnitude found in our prior work for the plastic flow stress of PMMA glass under constant strain rate conditions in the absence of aging and rejuvenation [31,35]. However, the temperature dependence of the plastic flow stress is very different than τ_{dy} which is relevant to a long-time creep experiment.

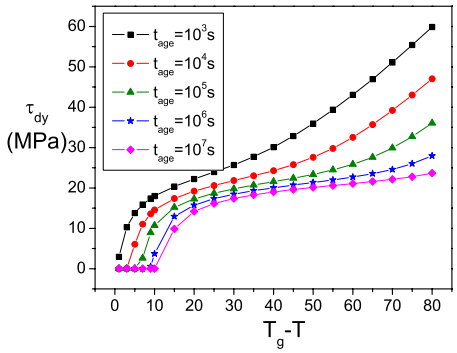

FIG. 5. (Color online) Dynamic yield stress (MPa) as a function of quench depth for five preaging times.

C. Nonequilibrium steady state

The nonequilibrium steady state ($t \to \infty$) is rigorously independent of preaging time and thermal history and reflects a competition between aging and stress-induced disordering. Figure 6 shows steady-state values of the density fluctuation amplitude ($S_{0,\infty}$) and relaxation time ($\tau_{\alpha,\infty}$) as a function of stress. The stress dependence of $S_{0,\infty}$ is sigmoidal for all temperatures. The intermediate stress transition region that separates the zero stress plateau (equilibrium value) and high stress steady-state nonequilibrium value is roughly independent of temperature despite the fact the two limiting density fluctuation amplitudes are increasingly different as the glass becomes colder. The percentage change in S_0 due to mechanical driving varies from ~6% at the highest temperature to ~50% at the lowest temperature. The steady-state relaxation time has also a roughly sigmoidal dependence on stress, but the absolute changes are massively larger. In the low and high stress regimes the relaxation time is roughly an exponentially decreasing function of stress, with a higher apparent slope in the low stress regime.

D. Time-dependent creep

Calculations of the time-dependent strain under fixed preaging and temperature but variable constant stress, and fixed

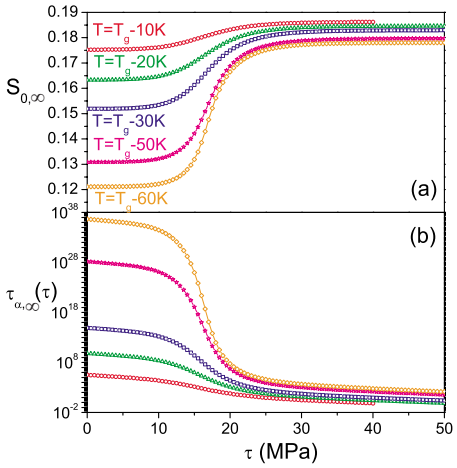

FIG. 6. (Color online) Stress dependence of the steady-state values of (a) the density fluctuation amplitude, $S_{0,\infty}$, and (b) mean relaxation time, $\tau_{\alpha,\infty}(\tau)$. Temperature increases from top to bottom in (a) and from bottom to top in (b).

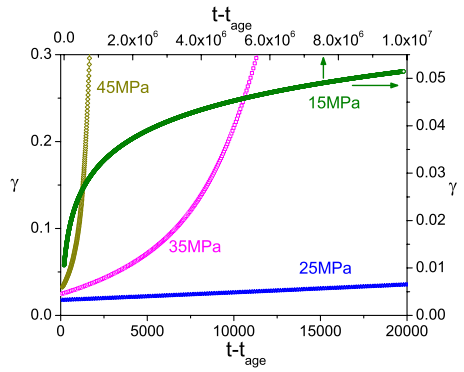

FIG. 7. (Color online) Dynamic strain creep curves as a function of elapsed time for four stresses and a fixed quench depth of $T_g - T = 50$ K and preaging time $t_{age} = 10^5$ s. The x and y axes of the concave-down curve is on the top and right, respectively. Corresponding time-evolution curves of the mean relaxation time can be found in Fig. 4(b).

stress and temperature but variable preaging time, are shown in Figs. 7 and 8, respectively. As stress increases, the temporal evolution of strain in Fig. 7 qualitatively changes from concave down with a quasiplateau, to nearly linear, to strongly concave up. These different behaviors reflect, respectively, dominance of aging, balance of aging and rejuvenation, and dominance of mechanical disordering (stress-induced flow). An analogous three-regime behavior is predicted for the segmental relaxation time [Fig. 4(b)]. The constant stress but variable preaging time results in Fig. 8 show a similar qualitative evolution of strain and τ_α, with aging dominant at short preaging times and mechanical rejuvenation dominant at long preaging times.

The creep strain rate under long time steady-state viscous flow conditions is shown in Fig. 9 as a function of stress for several quench depths. The limiting strain rate becomes

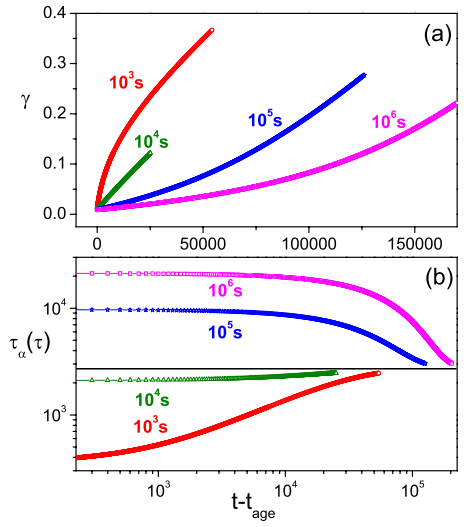

FIG. 8. (Color online) (a) Creep curves at four different preaging times for $T_g - T = 10$ K and a stress $\tau = 14$ MPa. The corresponding time-evolution curves of relaxation time are shown in (b). The black horizontal curve is the nonequilibrium steady state alpha time, $\tau_{\alpha,\infty}(\tau)$.

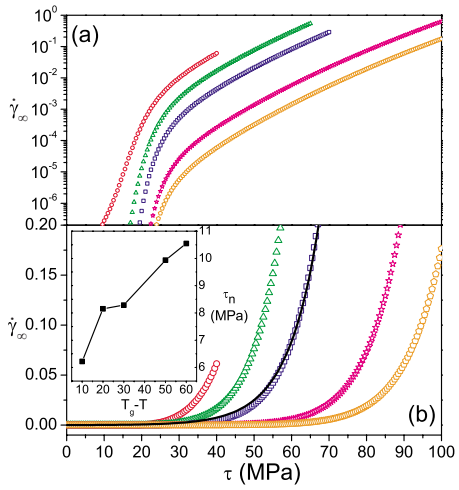

FIG. 9. (Color online) (a) Log-linear and (b) linear-linear plots of the steady state strain rate as a function of stress for $T = T_g - 10$ K, $T_g - 20$ K, $T_g - 30$ K, $T_g - 50$ K, and $T_g - 60$ K from left to right (red to orange). The black line in (b) shows an exponential fit for $T_g - 30$ K, i.e., $\dot{\gamma}_\infty \propto \exp(\tau/\tau_n)$. The inset of (b) shows the temperature dependence of the fitting parameter τ_n.

smaller as the glass becomes colder. The overall shape of the log-linear plot in Fig. 9(a) consists of two regimes: a steep increase from very small values $\dot{\gamma}_\infty$ at low stresses where the glass has a very high viscosity, which then changes to an exponential growth to large (eventually unbounded corresponding to flow) values with a high stress slope that gently decreases with cooling. Note that the crossover becomes broader as the glass becomes colder. Figure 9(b) shows the same results in a linear-linear format. At high strain rates, an exponential stress dependence describes the computations well: $\dot{\gamma}_\infty \propto \exp(\tau/\tau_n)$. The characteristic stress, τ_n, deduced from fitting our numerical calculations grows roughly linearly with cooling [inset of Fig. 9(b)], as predicted previously for the linear modulus and dynamic and absolute yield stresses in a constant rate experiment [31,34,35]. The magnitude of τ_n is modest, of order 5–10 MPa, far below the linear modulus and also generally smaller than the yield stresses that characterize constant rate experiments [31,35].

V. DISCUSSION

We have extended our previous statistical mechanical theories of polymer glasses based on activated hopping [29–37] to describe the coupled effects of physical aging, mechanical rejuvenation and thermal history on segmental relaxation, density fluctuations, and nonlinear mechanics. A number of bold approximations have been made, but no new parameters have been introduced relative to our prior predictive approach except for the one numerical prefactor in Eq. (16). The theory makes testable predictions for the time evolution and nonequilibrium steady-state values of the segmental relaxation time, density fluctuation amplitude, elastic modulus, etc. A rich dependence on preaging time, applied stress, and temperature occurs that reflects the nonlinear competition between aging and mechanical disordering.

Thermal history (preaging) is erased in the nonequilibrium steady state, although the properties of the latter do not correspond to a literal "fully rejuvenated" freshly quenched glass.

We briefly comment on several issues not addressed in detail in this paper that are of great interest in polymer glasses and which relate to some of our prior and present work. A hallmark of polymer glass phenomenology is "time-aging time" superposition of the dynamical shift factor as deduced from creep compliance measurements [8]. We have previously shown that this behavior is predicted by our theory in the context of the stress relaxation modulus [29,30]. We also showed that our theory of nonlinear creep in the absence of aging predicts collapse of compliance curves via horizontal shifting along the log-time axis [32]. Studying this question for creep with aging remains to be done, but we suspect such a superposition will be predicted. A second rather mysterious phenomenon, observed in both experiment and simulation, is the stress dependence of the apparent aging exponent measured in creep deformations, an effect sometimes called rejuvenation [8,17]. Specifically, the aging exponent decreases with applied stress. This phenomenon will be studied in depth in future work, but our results in insets B of Figs. 1–4 are of qualitative relevance. Note that the theory does predict that the effective aging exponent, μ, can decrease with applied stress. For example, in Fig. 1(b), $\mu \sim 0.68$, 0.64, and 0.57 for applied stresses of 0, 0.8, and 12 MPa, respectively. Also, the aging exponent does go to zero at what we call the "bifurcation stress." Moreover, μ can even become negative at larger stresses where mechanical disordering wins in determining the long-time nonequilibrium steady state. Perhaps this latter behavior is related to a phenomenon called "overaging" or "stress aging" where segmental mobility is *enhanced* under deformation, typically at rather low temperatures [66].

The present work provides the foundation for a quantitative treatment of both constant strain rate and constant stress (creep) polymer glass experiments. As will be reported in future articles, how preaging, aging during deformation, and mechanical disordering combine to determine the experimental yield stress (overshoot or peak in the stress versus strain curve), the strain softening phenomenon, plastic flow stress, and large strain upturn in creep can now be determined. Our preliminary results do capture the overshoot (yield peak) phenomenon often observed for a constant strain rate deformation, which emerges as a consequence of the competition between aging and mechanical rejuvenation. The detailed behavior of this yield peak depends on the preaging time, temperature quench depth, and strain rate in a manner that is consistent with experiment. Upon extension of the theory to include strain hardening in the presence of aging and rejuvenation, the remarkably rich experimental observations of Lee and co-workers [11–15] can be fully understood.

Finally, we mention a few other open problems and limitations of the present theory. There remains the question of the role of dynamic heterogeneity [67] as manifested, for example, by a relaxation time distribution, and how such heterogeneity is modified in a stressed and/or aging glass. Although polymer glass experiments find that postyield deformation strongly reduces heterogeneity as indicated by a narrowing of the relaxation time spectrum [11,14], computer simulations [14,17–19] that do not capture this aspect nevertheless account very well for essentially all the other observations. This raises the nontrivial question, of general interest above and below T_g, of how important dynamic heterogeneity is for understanding specific relaxation and mechanical phenomena. Within the NLE approach, two sources of dynamic heterogeneity (DH) have been previously discussed and analyzed for colloidal suspensions and hard-sphere fluids [24,25,36,68]. The first arises even when the dynamic free energy is uniquely defined since activated barrier hopping is a noise driven process. The latter results in "temporal" DH and a Poissonian distribution of alpha relaxation times [24]. A second possible origin of DH is based on a commonly employed quasistatic domain model which recognizes that the amplitude of density fluctuations (the key structural variable, S_0) is a distributed quantity on any finite length scale relevant to an activated dynamical process [68]. This "static disorder" is a structural mechanism for DH via fluctuations of the barrier height, again resulting in a relaxation time distribution. Exploring the consequences of these two DH mechanisms for the nonlinear mechanical and aging response of polymer glasses is an important problem for future study.

Finally, one can ask, "What are the limitations of using only one structural order parameter (S_0) in the stressed and aging glass?" It appears that an understanding of the Kovacs "memory effect" [69] associated with subjecting a glass to a complex thermal history requires at least one more dynamic order parameter, e.g., a dynamic effective temperature as in the recent work of Bouchbinder and Langer [70] or a distribution of relaxation times [8]. This issue needs careful future study within the NLE approach.

ACKNOWLEDGMENTS

The early stages of this work were performed at Illinois and funded by NSF-NIRT Project No. 0505840. Present support (K.S.S.) is from the Basic Energy Sciences, Division of Materials Science and Engineering, United States Department of Energy via Oak Ridge National Laboratory. K.S.S. acknowledges partial support during his stay at the Kavli Institute of Theoretical Physics in the context of the "Physics of Glasses" workshop (KITP is supported by NSF Grant No. NSF-PHY05-51164). We acknowledge many useful discussions with Mark Ediger, Jim Langer, Juan dePablo, and Jim Caruthers.

[1] K. L. Ngai, J. Non-Cryst. Solids **275**, 7 (2000).
[2] C. M. Roland, Soft Matter **4**, 2316 (2008).
[3] K. L. Ngai and D. J. Plazek, Rubber Chem. Technol. **68**, 376 (1995).
[4] G. B. McKenna, in *Comprehensive Polymer Science*, edited by C. Booth and C. Price (Pergamon, Oxford, 1990), Vol. 2, p. 311.
[5] F. T. Oyerokun and K. S. Schweizer, J. Chem. Phys. **123**, 224901 (2005).
[6] M. Rubinstein and R. H. Colby, *Polymer Physics* (Oxford Press, Oxford, 2003).
[7] I. M. Ward and D. M. Hadley, *Introduction to Mechanical Properties of Solid Polymers* (Wiley, New York, 1993).
[8] L. C. E. Struik, *Physical Aging in Amorphous Polymers and Other Materials* (Elsevier, Amsterdam, 1978).
[9] H. Meijer and L. E. Govaert, Prog. Polym. Sci. **30**, 915 (2005).
[10] R. N. Haward and R. J. Young, *The Physics of Glassy Polymers* (Chapman and Hall, London, 1997).
[11] H. N. Lee, K. Paeng, S. F. Swallen, and M. D. Ediger, Science **323**, 231 (2009).
[12] H. N. Lee, K. Paeng, S. F. Swallen, and M. D. Ediger, J. Chem. Phys. **128**, 134902 (2008).
[13] H. N. Lee, K. Paeng, S. F. Swallen, M. D. Ediger, R. A. Stamm, and J. M. Caruthers, J. Polym. Sci., Part B: Polym. Phys. **47**, 1713 (2009).
[14] R. A. Riggleman, H. N. Lee, M. D. Ediger, and J. J. de Pablo, Soft Matter **6**, 287 (2010).
[15] H. N. Lee and M. D. Ediger, Macromolecules **43**, 5863 (2010); J. Chem. Phys. **133**, 014901 (2010).
[16] J. Rottler and M. O. Robbins, Phys. Rev. E **68**, 011507 (2003).
[17] M. Warren and J. Rottler, Phys. Rev. E **76**, 031802 (2007).
[18] R. A. Riggleman, H. N. Lee, M. D. Ediger, and J. J. de Pablo, Phys. Rev. Lett. **99**, 215501 (2007).
[19] R. A. Riggleman, K. S. Schweizer, and J. J. de Pablo, Macromolecules **41**, 4969 (2008).
[20] R. S. Hoy and M. O. Robbins, Phys. Rev. E **77**, 031801 (2008).
[21] A. V. Lyulin, B. Vorselaars, M. A. Mazo, N. K. Balabaev, and M. A. Michels, Europhys. Lett. **71**, 618 (2005).
[22] K. S. Schweizer and E. J. Saltzman, J. Chem. Phys. **119**, 1181 (2003).
[23] K. S. Schweizer, J. Chem. Phys. **123**, 244501 (2005).
[24] K. S. Schweizer, Curr. Opin. Colloid Interface Sci. **12**, 297 (2007).
[25] E. J. Saltzman and K. S. Schweizer, Phys. Rev. E **77**, 051504 (2008).
[26] K. S. Schweizer and E. J. Saltzman, J. Chem. Phys. **121**, 1984 (2004).
[27] E. J. Saltzman and K. S. Schweizer, J. Chem. Phys. **121**, 2001 (2004).
[28] E. J. Saltzman and K. S. Schweizer, J. Phys.: Condens. Matter **19**, 205123 (2007).
[29] K. Chen and K. S. Schweizer, Phys. Rev. E **78**, 031802 (2008).
[30] K. Chen and K. S. Schweizer, Phys. Rev. Lett. **98**, 167802 (2007).
[31] K. Chen and K. S. Schweizer, Macromolecules **41**, 5908 (2008).
[32] K. Chen, K. S. Schweizer, R. Stamm, E. Lee, and J. M. Caruthers, J. Chem. Phys. **129**, 184904 (2008).
[33] K. Chen and K. S. Schweizer, Phys. Rev. Lett. **102**, 038301 (2009).
[34] K. Chen and K. S. Schweizer, J. Chem. Phys. **126**, 014904 (2007).
[35] K. Chen and K. S. Schweizer, EPL **79**, 26006 (2007).
[36] K. Chen, E. J. Saltzman, and K. S. Schweizer, J. Phys.: Condens. Matter **21**, 503101 (2009).
[37] K. Chen, E. J. Saltzman, and K. S. Schweizer, Annu. Rev. Condens. Matter Phys. **1**, 277 (2010).
[38] J. S. Langer, Phys. Rev. E **77**, 021502 (2008); **70**, 041502 (2004); J. S. Langer and L. Pechenik, *ibid.* **68**, 061507 (2003).
[39] T. R. Kirkpatrick and P. G. Wolynes, Phys. Rev. A **35**, 3072 (1987).
[40] V. N. Novikov and A. P. Sokolov, Phys. Rev. E **67**, 031507 (2003).
[41] P. G. Debenedetti and F. H. Stillinger, Nature (London) **410**, 259 (2001).
[42] F. H. Stillinger, P. G. Debenedetti, and S. Sastry, J. Chem. Phys. **109**, 3983 (1998).
[43] H. Eyring, J. Chem. Phys. **4**, 283 (1936).
[44] M. J. Osborne and D. J. Lacks, J. Phys. Chem. B **108**, 19619 (2004).
[45] D. L. Malandro and D. J. Lacks, J. Chem. Phys. **110**, 4593 (1999).
[46] M. Fuchs and M. E. Cates, Faraday Discuss. **123**, 267 (2003).
[47] P. Sollich, F. Lequeux, P. Hebraud, and M. E. Cates, Phys. Rev. Lett. **78**, 2020 (1997).
[48] V. Kobelev and K. S. Schweizer, Phys. Rev. E **71**, 021401 (2005).
[49] J. M. Caruthers, D. B. Adolf, R. S. Chambers, and P. Shrikhande, Polymer **45**, 4577 (2004).
[50] F. Ritort and P. Sollich, Adv. Phys. **52**, 219 (2003).
[51] J. P. Garrahan and D. Chandler, Proc. Natl. Acad. Sci. U.S.A. **100**, 9710 (2003).
[52] D. Chandler and J. P. Garrahan, Annu. Rev. Phys. Chem. **61**, 191 (2010).
[53] F. Spaepen, Acta Metall. **25**, 407 (1977).
[54] A. S. Argon, Acta Metall. **27**, 47 (1979).
[55] G. S. Grest and M. H. Cohen, Adv. Chem. Phys. **48**, 455 (1981).
[56] D. Rodney and C. A. Schuh, Phys. Rev. B **80**, 184203 (2009).
[57] E. Bouchbinder and J. S. Langer, Phys. Rev. E **80**, 031131 (2009).
[58] L. C. E. Struik, Polymer **38**, 4053 (1997).
[59] P. Coussot, Q. D. Nguyen, H. T. Huynh, and D. Bonn, Phys. Rev. Lett. **88**, 175501 (2002); P. C. F. Møller, J. Mewis, and D. Bonn, Soft Matter **2**, 274 (2006).
[60] Two relevant caveats are the following: (i) the freshly quenched state is not unique since it depends on cooling rate (a minor effect) and (ii) it is possible that the fully rejuvenated state corresponds to an effective temperature (or degree of disorder) above T_g, perhaps as high as the mode coupling or onset temperature.
[61] E. Munch, J. M. Pelletier, B. Sixou, and G. Vigier, Phys. Rev. Lett. **97**, 207801 (2006); L. David, G. Vigier, S. Etienne, A. Faivre, C. L. Soles, and A. F. Yee, J. Non-Cryst. Solids **235-237**, 383 (1998).

[62] H. A. Hristov, B. Bolan, A. F. Yee, L. Xie, and D. W. Gidley, Macromolecules **29**, 8507 (1996), and references cited therein.
[63] T. Egami, JOM **62**, 70 (2010).
[64] G. B. McKenna, J. Phys.: Condens. Matter **15**, S737 (2003).
[65] The PMMA compressibility and density data [26,27] above T_g yield the parameters $A \cong 0.693$ and $B \cong 1134$ K that quantify the equilibrium $S_0(T)$. Requiring the theory quantitatively reproduces [34] the typical experimental values of T_c (426 K) and T_g (378 K) as defined by $\tau_\alpha(T_g)=100$ s fixes $\rho\sigma^3=0.92$ and $a_c \cong 5$ in Eq. (4). In the glass state, the frozen density fluctuation parameter in Eq. (6) is fixed at $b=2/3$, a value consistent with scattering experiments [34]. The statistical segment length is fixed at $\sigma=1$ nm.
[66] E. T. J. Klompen, T. A. P. Engels, L. E. Govaert, and H. E. H. Meijer, Macromolecules **38**, 6997 (2005).
[67] M. D. Ediger, Annu. Rev. Phys. Chem. **51**, 99 (2000); R. Richert, J. Phys.: Condens. Matter **14**, R703 (2002).
[68] K. S. Schweizer and E. J. Saltzman, J. Phys. Chem. B **108**, 19729 (2004).
[69] A. J. Kovacs, Fortschr. Hochpolym.-Forsch. **3**, 394 (1964).
[70] E. Bouchbinder and J. S. Langer, Soft Matter **6**, 3065 (2010).